

Quenching of the E 2 phonon line in the Raman spectra of wurtzite GaAs nanowires caused by the dielectric polarization contrast

M. Ramsteiner, O. Brandt, P. Kusch, S. Breuer, S. Reich, and L. Geelhaar

Citation: *Applied Physics Letters* **103**, 043121 (2013); doi: 10.1063/1.4817078

View online: <http://dx.doi.org/10.1063/1.4817078>

View Table of Contents: <http://scitation.aip.org/content/aip/journal/apl/103/4?ver=pdfcov>

Published by the *AIP Publishing*

Articles you may be interested in

[Surface optical phonons in GaAs nanowires grown by Ga-assisted chemical beam epitaxy](#)

J. Appl. Phys. **115**, 034307 (2014); 10.1063/1.4862742

[Conduction band structure in wurtzite GaAs nanowires: A resonant Raman scattering study](#)

Appl. Phys. Lett. **100**, 073102 (2012); 10.1063/1.3684837

[Thermal conductivity of GaAs nanowires studied by micro-Raman spectroscopy combined with laser heating](#)

Appl. Phys. Lett. **97**, 263107 (2010); 10.1063/1.3532848

[Incorporation of the dopants Si and Be into GaAs nanowires](#)

Appl. Phys. Lett. **96**, 193104 (2010); 10.1063/1.3428358

[Structural characterization of GaAs and InAs nanowires by means of Raman spectroscopy](#)

J. Appl. Phys. **104**, 104311 (2008); 10.1063/1.3026726

The logo for AIP APL Photonics is displayed in a white font on a red background. The letters 'AIP' are large and bold, followed by a vertical bar and the words 'APL Photonics' in a smaller font.

APL Photonics is pleased to announce
Benjamin Eggleton as its Editor-in-Chief



Quenching of the E_2^H phonon line in the Raman spectra of wurtzite GaAs nanowires caused by the dielectric polarization contrast

M. Ramsteiner,^{1,a)} O. Brandt,¹ P. Kusch,² S. Breuer,^{1,b)} S. Reich,² and L. Geelhaar¹

¹Paul-Drude-Institut für Festkörperelektronik, Hausvogteiplatz 5–7, 10117 Berlin, Germany

²Fachbereich Physik, Freie Universität Berlin, Arnimallee 14, 14195 Berlin, Germany

(Received 14 June 2013; accepted 16 July 2013; published online 26 July 2013)

We investigate the Raman intensity of E_2^H phonons in wurtzite GaAs nanowire ensembles as well as single nanowires as a function of excitation wavelength. For nanowires with radii in the range of 25 nm, an almost complete quenching of the E_2^H phonon line is observed for excitation wavelengths larger than 600 nm. The observed behavior is quantitatively explained by the dielectric polarization contrast for the coupling of light into the GaAs nanowires. Our results define the limits of Raman spectroscopy for the detection of the wurtzite phase in semiconductor nanowires.

© 2013 AIP Publishing LLC. [<http://dx.doi.org/10.1063/1.4817078>]

Semiconductor nanowires (NWs) have become an extensively studied object of research both because of their potential for electronic and optoelectronic applications as well as the interesting fundamental phenomena associated with their growth. In particular, III-As semiconductor NWs often consist of both the zincblende (ZB) and wurtzite (WZ) polytypes and form heterostructures with complex optical properties.^{1–4} Since the WZ phase is the metastable modification of III-As semiconductors, most of its fundamental properties are unknown. In the case of WZ GaAs, even the band gap is a topic of active research.^{1–21}

Raman spectroscopy is a widely used tool for the characterization of semiconductor NWs.^{15,20–28} In particular, the crystal structure of NWs is reflected in Raman spectra by the number and character of the observed phonon modes as well as by their frequencies. More specifically, for the differentiation between ZB and WZ GaAs, the detection of the E_2^H phonon line can be used as a fingerprint for the WZ phase.²⁹ However, for optical excitation through the side facets of WZ NWs grown along the c -direction, the E_2^H phonon line can only be observed for incoming laser light polarized perpendicular to the NW axis.²⁹ At the same time, exactly this kind of linearly polarized light suffers from a vanishing optical transmission through NW side facets when the ratio-to-wavelength decreases below a certain value.^{30,31}

In this letter, we investigate the intensity of the E_2^H phonon line in Raman spectra of an as-grown GaAs NW ensemble and single nanowires as a function of the photon energy used for excitation. The experimental result is compared with calculations of the polarization-dependent optical extinction expected for the GaAs NW ensemble.

GaAs NWs were prepared by molecular-beam epitaxy (MBE) using Au-induced vapor-liquid-solid (VLS) growth on Si(111) substrates. Au droplets were prepared on the oxide-free substrate by deposition of a 0.6 Å thin Au layer and subsequent heating. The NWs were grown for 30 min at

500 °C under As-rich growth conditions with a flux ratio of $F_{As}/F_{Ga} = 2$. Figures 1(a) and 1(b) show high-resolution transmission electron microscopy (HREM) images of a single GaAs NW of this NW ensemble. The NW, which has grown along the c -axis, exhibits the WZ structure intersected by isolated stacking faults (SFs) as visible in the bottom of Fig. 1(a). The reflection-high energy diffraction (RHEED) pattern displayed in Fig. 1(c) demonstrates that the HREM images are representative for the entire ensemble, as the pattern exhibits the expected reflections for the WZ structure while reflections of the ZB structure are absent. These observations have been confirmed by x-ray diffraction and resonant Raman scattering as reported in Refs. 3 and 20.

A statistical analysis of several scanning electron micrographs yields an average NW density of $1.3 \times 10^9 \text{ cm}^{-2}$, an average length of about 2 μm , and a mean radius of $(23.7 \pm 6.4) \text{ nm}$. For single-wire measurements, NWs were harvested from the Si substrate by ultrasonication in ethanol and subsequently dispersed on a Si wafer. Raman measurements were performed at room temperature using either the tunable fundamental or frequency-doubled output of a Ti:sapphire ring laser, or the discrete lines of Ar^+ and Kr^+

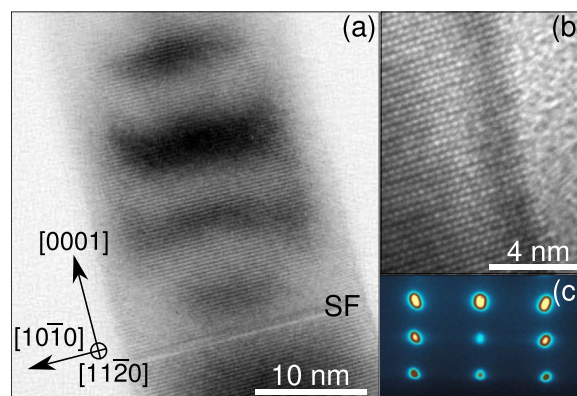


FIG. 1. (a) HREM image of a single GaAs NW of the ensemble under investigation. The basal planes and a SF are clearly visible. (b) Lattice image taken from the same NW resolving the WZ structure along the $[11\bar{2}0]$ zone axis. (c) RHEED pattern of the GaAs NW ensemble along the $[11\bar{2}0]$ azimuth. No reflections pertinent to the ZB structure are observed.

^{a)}Author to whom correspondence should be addressed. Electronic mail: ramsteiner@pdi-berlin.de

^{b)}Present address: Department of Electronic Materials Engineering, Research School of Physics and Engineering, The Australian National University, Canberra, ACT 0200, Australia

ion lasers as excitation. The respective laser line was focused onto the sample by a microscope objective. The scattered signal was collected by the same objective and dispersed spectrally by a Horiba 64-cm triple spectrograph or a 80-cm single monochromator. The signal was recorded using a LN₂-cooled CCD. For single, dispersed GaAs NWs the measurements were performed in backscattering geometry perpendicular to the NWs' *c*-axis and with a well defined polarization with respect to the *c*-axis. Measurements of the NW ensemble, in contrast, were performed from the as-grown sample in backscattering geometry along to the NWs' *c*-axis.

Figure 2 displays Raman spectra of the GaN NW ensemble excited at three different wavelengths. All spectra display longitudinal optical (LO) and transverse optical (TO) phonon lines (292 and 268 cm⁻¹) as well as the E₂^H phonon line (258 cm⁻¹). The TO and LO phonon lines originate both from ZB and WZ sections of the GaAs NWs since either of their frequency is too close to be resolved in these spectra. The high intensity of the E₂^H phonon line for excitation at 461.9 nm reflects the dominating contribution of the WZ phase in the NWs. The most striking observation, however, is the progressive quenching of the E₂^H phonon line when increasing the excitation wavelength to 501.6 and 647.1 nm.

Raman spectra of a single NW are shown in Fig. 3 for excitation at 413.1 and 632.8 nm. In this case, the laser was focused onto a NW side facet and linearly polarized perpendicular to the NW axis (TE polarization). For this well-defined scattering geometry, the quenching of the E₂^H phonon line is found to be essentially complete compared with the experimental result obtained from the NW ensemble depicted in Fig. 2.

For an understanding of these observations, we consider the following arguments. Even for Raman backscattering along the NW's *c*-axis it has been found that light enters and leaves the NWs mainly through their side facets with a considerable contribution of wavevectors nearly perpendicular to the NWs' *c*-axis.^{24,32} Due to this fact, the effective

scattering geometries are similar for the measurements on the NW ensemble (cf. Fig. 2) and the single dispersed NW (cf. Fig. 3). For this Raman configuration, scattering by E₂^H phonons is allowed only for incoming light polarized perpendicular to the NW axis (TE polarization).²⁹ Consequently, a potential explanation for the quenching of the E₂^H phonon line is the significant decrease in the transmission through the NW's side facets for light of exactly this polarization. In order to verify this hypothesis, we measured the intensity of the E₂^H Raman line for the NW ensemble as a function of the excitation wavelength and calculated the polarization-dependent optical extinction of the NWs taking into account both elastic scattering and absorption.^{30,31} For the calculations, we assumed the NWs to be surrounded by air (refractive index $n_{\text{Air}} = 1$) which is appropriate for the following comparison with experiments conducted on the as-grown NW ensemble. For NWs dispersed on another substrate, it may be necessary to take into account that one side facet of the NWs is attached to a surface of different material, particularly when the refractive index of this material is very different from that of air, such as in the case of metals.

In contrast to the case of E₂^H phonons, Raman scattering by TO phonons (A₁ as well as E₁ type) is allowed by selection rules for light polarized parallel to the *c*-axis and backscattering through the NWs' side facets (TM polarization).²⁹ Hence, the E₂^H/TO intensity ratio is a suitable measure for the ratio between the TE and TM polarized optical extinction by the NWs. Figure 4 shows the measured E₂^H/TO intensity ratio as a function of the excitation wavelength. The TE/TM intensity ratio of the optical extinction has been calculated using the formalism described in Refs. 30 and 31 for GaAs nanowires with radii between 18 and 22 nm, i.e., for values which are within the range of radii obtained by scanning electron microscopy. Using the complex dielectric function for GaAs given in Ref. 33, the calculated TE/TM ratio reproduces the experimentally measured Raman intensity ratio well. This agreement suggests that the quenching of the E₂^H phonon line for excitation wavelengths approaching 650 nm

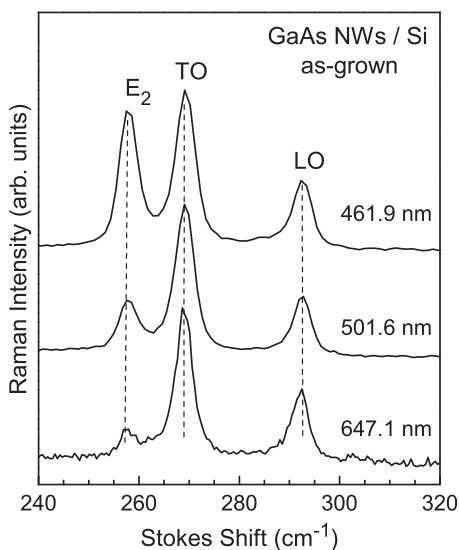


FIG. 2. Raman spectra (spectral resolution: 3 cm⁻¹) of the GaAs NW ensemble excited at three different wavelengths as indicated in the figure. The spectra have been normalized to the TO-phonon peak intensity.

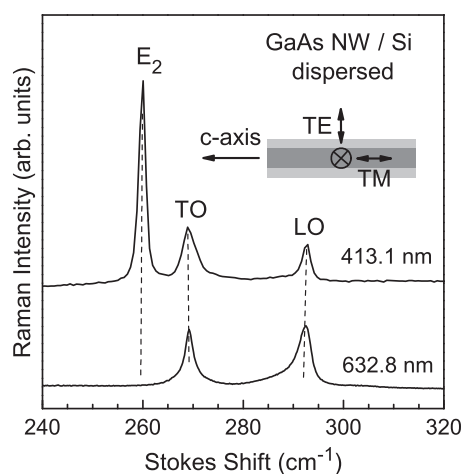


FIG. 3. Raman spectra (spectral resolution: 1 cm⁻¹) of a single GaAs NW dispersed onto a Si wafer excited at two different wavelengths as indicated in the figure. The light was linearly polarized perpendicular to the NW *c*-axis (TE polarization). The measurement configuration is shown schematically in the inset of the figure. The spectra have been normalized to the TO-phonon peak intensity.

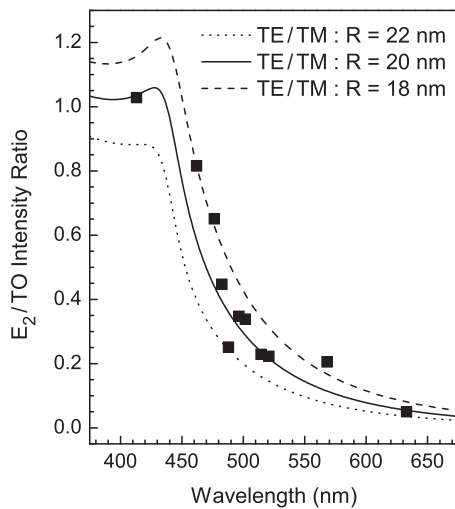


FIG. 4. Raman intensity of scattering by E_2^H phonons normalized to that of scattering by TO phonons for the GaAs NW ensemble as a function of excitation wavelength (full squares) together with the calculated TE/TM intensity ratio of the optical extinction. The NW radii used for the calculation are indicated in the figure. The theoretical curves are scaled by a factor of 1.85 in order to take into account the different efficiencies for scattering by E_2^H and TO phonons.

is indeed induced by the vanishing optical transmission for TE polarized light. Furthermore, our findings confirm that even for backscattering along the c -axis light coupling in NW ensembles occurs mainly through the NW side facets.^{24,32}

As a consequence of our findings, the ability of Raman scattering to detect the WZ phase in a GaAs NW ensemble strongly depends on the wavelengths used for excitation. This dependence is reviewed in Fig. 5. The main panel displays the calculated TE/TM ratio of the optical extinction as a function of the NW radius for different wavelengths. In order to obtain the reversed information, we defined a critical radius (R_C) below which the TE/TM ratio becomes smaller than 50%. The dependence of this critical radius on the optical wavelength is displayed in the inset of Fig. 5. When using a He-Ne laser for excitation (wavelength of 632.8 nm),

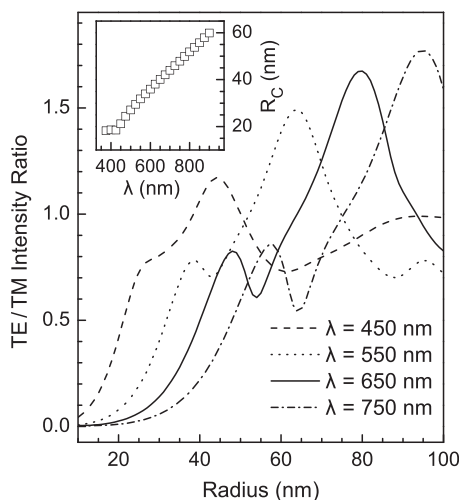


FIG. 5. TE/TM intensity ratio of the optical extinction as a function of the NW radius for different optical wavelengths (450 nm: dashed line, 550 nm: dotted line, 650 nm: solid line, 750 nm: dashed-dotted line). The inset displays the critical radius R_C as a function of the optical wavelength.

for example, the presence of the WZ phase is detected via scattering by E_2^H phonons only for NWs with radii above 40 nm.

A wavelength-dependent quenching of E_2 phonon modes has also been observed for bulk CdS in the WZ modification.³⁴ In this case, however, the vanishing Raman intensity is caused by an antiresonance in the scattering efficiency. This same explanation does not hold for our results, since a strong E_2^H phonon line has been observed from WZ GaAs needles of large radii (in the range of 500 nm) in Raman spectra excited at wavelengths as long as 825 nm.²⁶ In contrast, for excitation in the wavelength range between 700 and 900 nm we have not been able to detect the E_2^H phonon mode in Raman spectra of WZ GaAs NWs with radii of about 25 nm. The strong dielectric contrast inhibits the transmission of TE polarized light as expected from the electrodynamic model depicted in Fig. 5.

Finally, our results demonstrate that, in general, great care has to be taken in the analysis and interpretation of polarization-dependent Raman data from NWs. Furthermore, our findings also have implications for the spontaneous and stimulated emission from semiconductor NWs. In fact, the emission related to the lowest-energy valence band in WZ semiconductors is strongly polarized perpendicular to the c -axis,^{35,36} and is thus subject to the same effects discussed here for Raman scattering. The dielectric polarization contrast may thus seriously affect the efficiency of light-emitting NW devices based on WZ material.

We are indebted to A. Trampert for transmission electron microscopy and U. Jahn for the critical reading of the manuscript. Parts of this work were supported by the ERC under Grant No. 210642.

- ¹D. Spirkoska, J. Arbiol, A. Gustafsson, S. Conesa-Boj, F. Glas, I. Zardo, M. Heigoldt, M. H. Gass, A. L. Bleloch, S. Estrade, M. Kaniber, J. Rossler, F. Peiro, J. R. Morante, G. Abstreiter, L. Samuelson, and A. Fontcuberta i Morral, *Phys. Rev. B* **80**, 245325 (2009).
- ²M. Heiss, S. Conesa-Boj, J. Ren, H. H. Tseng, A. Gali, A. Rudolph, E. Uccelli, F. Peiró, J. Ramon Morante, D. Schuh, E. Reiger, E. Kaxiras, J. Arbiol, and A. Fontcuberta i Morral, *Phys. Rev. B* **83**, 045303 (2011).
- ³U. Jahn, J. Lähnemann, C. Pfüller, O. Brandt, S. Breuer, B. Jenichen, M. Ramsteiner, L. Geelhaar, and H. Riechert, *Phys. Rev. B* **85**, 045323 (2012).
- ⁴A. M. Graham, P. Corfdir, M. Heiss, S. Conesa-Boj, E. Uccelli, A. Fontcuberta i Morral, and R. T. Phillips, *Phys. Rev. B* **87**, 125304 (2013).
- ⁵M. Murayama and T. Nakayama, *Phys. Rev. B* **49**, 4710 (1994).
- ⁶F. Martelli, M. Piccin, G. Bais, F. Jabeen, S. Ambrosini, S. Rubini, and A. Franciosi, *Nanotechnology* **18**, 125603 (2007).
- ⁷Z. Zanolli, F. Fuchs, J. Furthmüller, U. von Barth, and F. Bechstedt, *Phys. Rev. B* **75**, 245121 (2007).
- ⁸M. Moewe, L. C. Chuang, S. Crankshaw, C. Chase, and C. Chang-Hasnain, *Appl. Phys. Lett.* **93**, 023116 (2008).
- ⁹T. B. Hoang, A. F. Moses, H. L. Zhou, D. L. Dheeraj, B.-O. Fimland, and H. Weman, *Appl. Phys. Lett.* **94**, 133105 (2009).
- ¹⁰A. De and C. E. Pryor, *Phys. Rev. B* **81**, 155210 (2010).
- ¹¹T. B. Hoang, A. F. Moses, L. Ahtapodov, H. L. Zhou, D. L. Dheeraj, A. T. J. van Helvoort, B.-O. Fimland, and H. Weman, *Nano Lett.* **10**, 2927 (2010).
- ¹²G. Ihn, M.-Y. Ryu, and J.-I. Song, *Solid State Commun.* **150**, 729 (2010).
- ¹³M. Jancu, K. Gauthron, L. Largeau, G. Patriarche, J.-C. Harmand, and P. Voisin, *Appl. Phys. Lett.* **97**, 041910 (2010).
- ¹⁴B. V. Novikov, S. Yu. Serov, N. G. Filosofov, I. V. Shtrom, V. G. Talalaev, O. F. Vyvenko, E. V. Ubyivovk, Yu. B. Samsonenko, A. D. Bouravleuv, I. P. Soshnikov, N. V. Sibirev, G. E. Cirlin, and V. G. Dubrovskii, *Phys. Status Solidi (RRL)* **4**, 175 (2010).

- ¹⁵B. Ketterer, M. Heiss, E. Uccelli, J. Arbiol, and A. Fontcuberta i Morral, *ACS Nano* **5**, 7585 (2011).
- ¹⁶B. Ketterer, M. Heiss, M. J. Livrozet, A. Rudolph, E. Reiger, and A. Fontcuberta i Morral, *Phys. Rev. B* **83**, 125307 (2011).
- ¹⁷L. Ahtapodov, J. Todorovic, P. Olk, T. Mjåland, P. Slåttnes, D. L. Dheeraj, A. T. J. van Helvoort, B.-O. Fimland, and H. Weman, *Nano Lett.* **12**, 6090 (2012).
- ¹⁸A. Belabbes, C. Panse, J. Furthmuller, and F. Bechstedt, *Phys. Rev. B* **86**, 075208 (2012).
- ¹⁹R. Gurwitz, A. Tavor, L. Karpeles, I. Shalish, W. Yi, G. Seryogin, and V. Narayanamurti, *Appl. Phys. Lett.* **100**, 191602 (2012).
- ²⁰P. Kusch, S. Breuer, M. Ramsteiner, L. Geelhaar, H. Riechert, and S. Reich, *Phys. Rev. B* **86**, 075317 (2012).
- ²¹W. Peng, F. Jabeen, B. Jusserand, J. C. Harmand, and M. Bernard, *Appl. Phys. Lett.* **100**, 073102 (2012).
- ²²T. Livneh, J. P. Zhang, G. S. Cheng, and M. Moskovits, *Phys. Rev. B* **74**, 035320 (2006).
- ²³Q. Xiong, G. Chen, H. R. Gutierrez, and P. C. Eklund, *Appl. Phys. A* **85**, 299 (2006).
- ²⁴S. Lazić, E. Gallardo, J. Calleja, F. Agulló-Rueda, J. Grandal, M. Sánchez-García, E. Calleja, E. Luna, and A. Trampert, *Phys. Rev. B* **76**, 205319 (2007).
- ²⁵I. Zardo, S. Conesa-Boj, F. Peiro, J. R. Morante, J. Arbiol, E. Uccelli, G. Abstreiter, and A. Fontcuberta i Morral, *Phys. Rev. B* **80**, 245324 (2009).
- ²⁶S. Crankshaw, L. C. Chuang, M. Moewe, and C. Chang-Hasnain, *Phys. Rev. B* **81**, 233303 (2010).
- ²⁷E. O. Schäfer-Nolte, T. Stoica, T. Gotschke, F. Limbach, E. Sutter, P. Sutter, and R. Calarco, *Appl. Phys. Lett.* **96**, 091907 (2010).
- ²⁸E. Dimakis, M. Ramsteiner, A. Tahraoui, H. Riechert, and L. Geelhaar, *Nano Res.* **5**, 796 (2012).
- ²⁹H. Harima, *J. Phys.: Condens. Matter* **14**, R967 (2002).
- ³⁰R. Ruppin, *Opt. Commun.* **211**, 335 (2002).
- ³¹J. Giblin, V. Protasenko, and M. Kuno, *ACS Nano* **3**, 1979 (2009).
- ³²C. Pfüller, M. Ramsteiner, O. Brandt, F. Grosse, A. Rathsfeld, G. Schmidt, L. Geelhaar, and H. Riechert, *Appl. Phys. Lett.* **101**, 083104 (2012).
- ³³D. E. Aspnes and A. A. Studna, *Phys. Rev. B* **27**, 985 (1983).
- ³⁴T. C. Damen and J. F. Scott, *Solid State Commun.* **9**, 383 (1971).
- ³⁵P. Misra, O. Brandt, H. T. Grahn, H. Teisseyre, M. Siekacz, C. Skierbiszewski, and B. Łuczniak, *Appl. Phys. Lett.* **91**, 141903 (2007).
- ³⁶O. Brandt, P. Misra, T. Flissikowski, and H. T. Grahn, *Phys. Rev. B* **87**, 165308 (2013).